Welding in the World (2021) 66:93–103
https://doi.org/10.1007/s40194-021-01187-z

RESEARCH PAPER

Parameter investigation and optimization of friction stir welded AA6061/TiO_2 composites through TLBO

Subramanya R. Prabhu[1,2] · Arun Shettigar[2] · Mervin A. Herbert[2] · Shrikantha S. Rao[2]

Received: 8 September 2020 / Accepted: 13 September 2021 / Published online: 7 October 2021
© The Author(s) 2021, corrected publication 2022

Abstract
This paper explicates the joining of AA 6061/TiO_2 composites by the friction stir welding (FSW) process. FSW experiments were conducted as per the three factors, three-level, central composite ivy– face-centered design method. Mathematical relationships between the FSW process parameters, namely tool geometry, welding speed, and tool rotational speed, and the output responses such as hardness, yield strength, and ultimate tensile strength were established using response surface methodology. Adequacies of established models were assessed through the analysis of variance method. Further, the paper elucidates the application of the teaching–learning-based optimization (TLBO) algorithm to identify the optimal values of input variables and to obtain an FSW joint with superior mechanical properties. The optimized experimental condition obtained from the TLBO yields an FSW joint with a UTS of 174 MPa, yield strength of 120 MPa, and hardness of 126HV. The study revealed that the result of the TLBO algorithm matched the findings of the FSW experiments.

Keywords AA6061/TiO_2 composite · Friction stir welding · Response surface methodology · TLBO algorithm · Optimization

1 Introduction

As a solid-state thermo-mechanical joining technique, friction stir welding (FSW) is considered a promising method for welding aluminum matrix composites (AMCs) as it has the ability to eliminate the defects such as voids, porosity, and cracks associated with the traditional metal welding process [1]. FSW has been widely applied in many industrial applications including automotive, marine, aerospace, railway, and renewable energy [2]. FSW is a dynamically continuous joining method that operates at a temperature less than the melting point of the material to be welded. This offers superior welding characteristics in alloys and metal matrix composites and consumes lesser energy than the conventional fusion welding process [3, 4]. In FSW, a rotating tool is inserted into the faying surfaces of the parts to be welded, and the tool is made to move along the weld line. The non-consumable tool generates sufficient heat at the weld area to plasticize the material by developing a huge frictional force between the revolving tool and the stationary workpiece. The localized heating softens the material around the pin, and a combination of tool rotation and translation leads to the movement of material from the front of the pin to the back of the pin [5, 6]. Plasticized material flow in the FS region is affected by the relative motion of the tool concerning the workpiece as well as the tool pin geometry [7, 8]. During the FSW process, the heat developed at the weld zone is comparatively lower than the amount of heat supplied in the conventional fusion welding process, which minimizes distortion and subsequently reduces the residual stress. Thus, FSW yields a uniform, void and defect-free joint which makes it an attractive joining process in the automotive, aerospace, and marine industries [9].

During the recent decades, several experimental studies were reported in search of the impact of FSW process variables on the mechanical and metallurgical characteristics of aluminum matrix composites (AMCs) dispersed with

Recommended for publication by Commission XVIII - Quality Management in Welding and Allied Processes

✉ Subramanya R. Prabhu
subramanya.prabhu@manipal.edu

[1] Department of Mechatronics Engineering, Manipal Institute of Technology, Manipal Academy of Higher Education, Manipal, India

[2] Department of Mechanical Engineering, National Institute of Technology Karnataka, Mangalore, India

different particulates such as SiC, B_4C, ZrB_2, AlN, TiB_2, TiC, and rutile [10, 11]. Comprehensive literature reviews suggest that FSW is a potential method to weld AMCs. It has been inferred from the literature that the process parameters (welding and tool rotational speed, tool geometry, axial force, tool tilt angle, tool, and workpiece material) play an important role to attain sound [12, 13]. High-quality welds with superior properties can be obtained by choosing the relevant process variables with their optimum values. Several techniques exist to predict the optimum process parameters. Siva et al. [14] espoused a multi-criteria decision-making technique to evaluate the interrelationship among the FSW process parameters and different joint properties of the FS welded joints. The generalized reduced gradient (GRG) technique was utilized by Kalaiselvan and Murugan [15] to optimize the process variable in FSW of Al-B_4C composite and evaluate metallurgical characteristics of FS welded joints. Verma et al. [16] performed a desirability approach based on optimization of the FSW process variable of armor marine grade alloy and inferred that the joint strength was mainly affected by the tool rotational speed and less influenced by axial load and the welding speed. Taguchi-based Grey Relational Analysis (TGRA) technique was adopted by [17] for optimization of FSW parameters to join pure copper. The robustness of the GRA technique was tested by conducting the confirmation trials using optimum process variables. TOPSIS approach was used by Prabhu et al. [18] for multi-response optimization of the FSW process to join AMCs. The study revealed that the process parameter values obtained from this technique provided better closeness coefficient values. Abdel Maboud et al. [19] employed the analysis of variance (ANOVA) technique to identify the critical factors and used response surface methodology (RSM) to understand the influence of various FSW process parameters. Sreenivasan et al. [20] optimized the FSW of AA7075-SiC composite through a genetic algorithm by using fitness function and predicted maximum value of hardness and tensile strength. Recently, Parida and Pal [21] proposed a fuzzy-assisted Taguchi approach for optimizing parameters of the FSW process with multiple responses. A fuzzy inference system was adopted to convert multiple responses into a single objective, and optimization was carried out using the Taguchi technique. ANN with backpropagation algorithm was used by [22] for FSW of dissimilar alloys and performed multi-response optimization using particle swarm optimization (PSO) method. Prasanth et al. [23] applied the artificial bee colony (ABC) algorithm to evaluate the optimal combination of variables to attain better joint characteristics of FS welded dissimilar aluminum alloys.

From the available literature, it is learned that several traditional methods were used for the optimization of the FSW process, but these methods do not work well over a wider range of problems, and also often, they offer a local optimum solution. An evolutionary algorithm such as GA can overcome these limitations, but efficient usage of this technique depends on the size of the population and the diversity of each solution in the given problem. Other evolutionary algorithms such as ABC and PSO are adopted by researchers. But, successful usage of these techniques needs a proper selection of specific parameters related to the algorithm such as scaling, crossover, and mutation probability [24]. Choosing suitable algorithm-specific variables for a given problem is itself a major task in these optimization techniques. To eliminate these limitations, an algorithm-specific parameter-less algorithm is used in this work, developed by Rao et al. [25, 26] known as the TLBO algorithm. It employs only general controlling variables like several iterations and population size for its working.

Identifying the optimal FSW process parameters to join aluminum matrix composites is a critical issue in realizing the process. Consequently, there is a requirement to formulate the modeling and optimization strategies for joining of composite by the FSW process. Hence, this paper focuses on the joining of AMCs through the FSW technique and developing the mathematical models for different responses such as yield strength (YS) and ultimate tensile strength (UTS) and hardness using the RSM technique. Further, attempts were made to apply a novel TLBO algorithm to identify the optimal combination of process variables from the developed mathematical model. To the author's (of this paper) knowledge, the application of the TLBO algorithm to optimize the FSW of AA6061/TiO_2 composite has not been yet studied and reported in the literature. Hence, the present article tries to contribute to the related knowledge base on this matter.

In the present paper, firstly the detail of experiments conducted to join AA6061/TiO_2 composite by FSW process is explained, followed by the steps to develop a mathematical model between the input parameters and the output responses using RSM that is illustrated. Then the impact of process parameters on different outputs responses is explained. Furthermore, the comprehensive explanation on working and the application of the TLBO algorithm on the developed models are shown along with the confirmation trials, conducted to confirm the relevance of the algorithm for the present FSW process.

2 Experiment

Stir cast AA6061/TiO_2 composite plates have been considered in the present study. Table 1 lists the composition of the stir cast composite. The plates for welding were cut from the stir cast blocks in the size of $100 \times 50 \times 5$, and FSW of these plates was performed on a CNC milling machine (vertical milling center). FSW tool with three different types of pin

profiles was used in this study, namely square, triangle, and threaded cylindrical. Pin dimensions were chosen in such a way that all three pins cover the same dynamic volume during the FSW process. The tools are made of molybdenum steel, hardened to 63 HRC, having a 6 mm pin dynamic diameter and 4.7 mm pin length. Figure 1 depicts the tools used in the present work. Welding speed, tool rotational speed, and tool geometry are identified as process variables, whereas YS, UTS, and hardness are considered output responses.

The present study employed a central composite design (CCD) to fit a second-order response surface. CCD comprises a set of trial experiments at center points, a set of trial experiments in axial points, and a set of trial experiments in other points [22]. CCD consists of a set of trial experiments at axial points, at center points, and experiments at other points. Axial points provide an evaluation of curvature of output response surfaces, whereas center points reduce the error related to model prediction and deliver uniform precision, ensuring a similar variance of prediction in the response surface. This ensures protection against bias, due to the existence of higher-order coefficients [27]. Thus, the process stability, uniform precision, and variance of prediction are ensured by the center points in the design, and also these points provide a shield against bias. The number of trials to be performed in CCD is calculated by a formula (2^p+2p+q), where p represents the number of process variables or factors used in the study. The term q represents the number of central points, term $2p$ denotes axial points, and term 2^p is the number of trial experiments. For a process with three factors, the suggested number of central points is either five or six [28]. In most of the studies, the number of central points was taken as six, by considering the suggested values of q and available resources in the studies [29, 30]. Consequently, in the present work, the CCD matrix with three process variables or factors with three levels that are having 20 sets of experiments are designed to compute the linear, quadratic, and two-way interaction of the input process variables on the output responses. Twenty sets of coded experiments consist of 2^3 or 8 sets of trial experiments, 6 sets at axial points, and the remaining 6 sets at central points. Table 2 lists the coded values of input process parameters.

Specimen for UTS test was prepared as per the ASTM-E8 guidelines, by cutting the sample normal to the weld

Table 1 Chemical composition (in wt %) of the stir cast composite

Chromium	Copper	Iron	Manganese	Magnesium	Silicon	TiO_2	Aluminum
0.04–0.35	0.15–0.4	0.7	0.15	0.8–1.2	0.4–0.8	3	Remaining

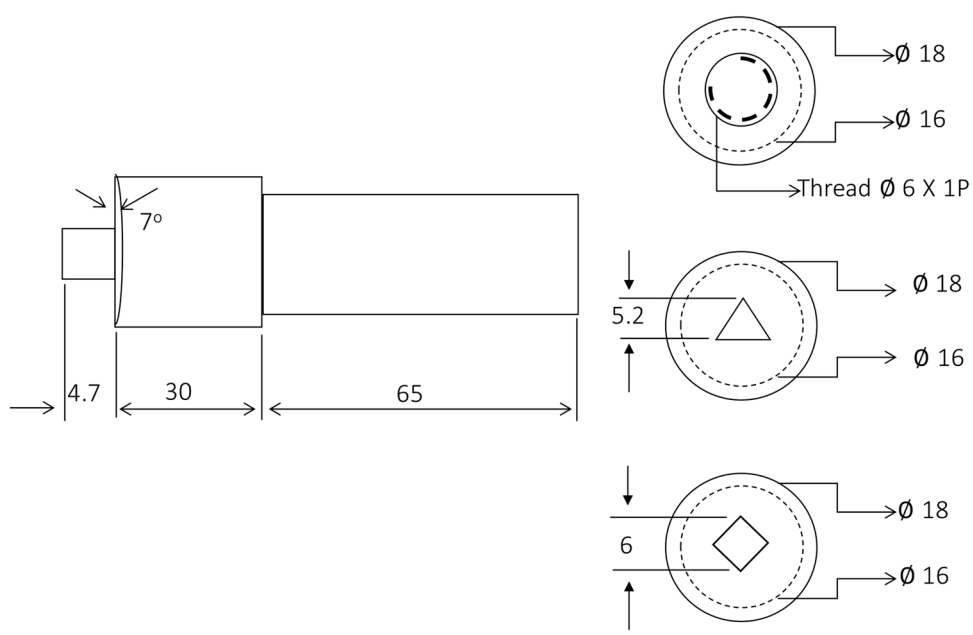

Fig. 1 FSW tool with square, triangle, and a threaded cylindrical pin

Table 2 Input process parameters with levels

Parameters	Low	Mid	High
Tool rotational speed (RS) (rpm)	750	1000	1250
Welding speed (WS) (mm/min)	60	75	90
Tool geometry (TG)	Threaded cylindrical (TC)	Triangle (TL)	Square (SQ)

direction as depicted in Fig. 2 and tested on a universal testing machine. For each of the experiments, three samples were taken for testing, and the mean of these test values was taken as final values. Measurement of hardness was done using Vickers hardness tester, with a load of indentation of 5 kg for 30 s. Measurement was done in the mid of the stir zone.

3 Development of a mathematical model

The process parameters and the output responses were correlated by developing a second-order regression equation, and the response function Z is mathematically represented as:

$$Z = Q_0 + Q_i x_i + Q_{ii} x_i^2 + Q_{ij} x_i x_j + er \quad (1)$$

where Q_0 denotes regression constant and Q_i, Q_{ii}, and Q_{ij} denote linear, quadratic, and interaction coefficients, respectively, whereas x_i and x_j represent the independent process parameters, Z denotes the dependent output response, and e_r represents the error in the experiments [31]. As the present work consists of three independent parameters, the above relation may be shown in the following form:

$$\begin{aligned} Output = {} & Q_0 + Q_1(RS) + Q_2(WS) + Q_3(TG) \\ & + Q_{11}(RS^2) + Q_{22}(WS^2) + Q_{33}(TG^2) \\ & + Q_{12}(RS.WS) + Q_{13}(RS.TG) \\ & + Q_{23}(WS.TG). \end{aligned} \quad (2)$$

where Q_0 is a constant; Q_1, Q_2, and Q_3 are linear coefficients; Q_{12}, Q_{13}, and Q_{23} are interaction coefficients; Q_{11}, Q_{22}, and Q_{33} are quadratic coefficients in the regression model; and RS, WS, and TG represent process parameters. Integer values are assigned to the different types of tool geometries to develop the mathematical model. TC, TL, and SQ are assigned integer values of 1, 1.5, and 2, respectively.

Minitab software was used to carry out regression analysis to obtain coefficients of the regression equation [32]. The mathematical relationships between the variables and the output responses were developed and given by Eqs. 3a, 3b, and 3c.

$$\begin{aligned} YS = {} & -257.5 + 0.5071 * RS + 1.975 * WS \\ & + 39.6 * TG - 0.000252 * RS * RS \\ & - 0.00990 * WS * WS - 12.91 * TG * TG \\ & - 0.000133 * RS * WS + 0.00200 * RS * TG \\ & + 0.0333 * WS * TG \end{aligned} \quad (3a)$$

$$\begin{aligned} UTS = {} & -354.2 + 0.7520 * RS + 2.049 * WS \\ & + 53.8 * TG - 0.000374 * RS * RS \\ & - 0.00828 * WS * WS - 15.45 * TG * TG \\ & - 0.000133 * RS * WS + 0.00000 * RS * TG \\ & + 0.0000 * WS * TG \end{aligned} \quad (3b)$$

$$\begin{aligned} Hardness = {} & -100.0 + 0.3196 * RS + 0.757 * WS \\ & + 26.1 * TG - 0.000165 * RS * RS \\ & - 0.00364 * WS * WS - 9.27 * TG * TG \\ & + 0.000033 * RS * WS + 0.00300 * RS * TG \\ & + 0.0500 * WS * TG \end{aligned} \quad (3c)$$

ANOVA technique is employed to test the adequacy of the developed empirical relationships. Table 3 lists the result

Table 3 ANOVA results

Response	Sum of squares	Mean square	F value	R^2	Adj R^2
YS	2325.85	258.428	162.07	99.32%	98.71%
UTS	4845.96	538.44	200.64	99.45%	98.95%
Hardness	1071.47	119.052	64.23	98.30%	96.77%

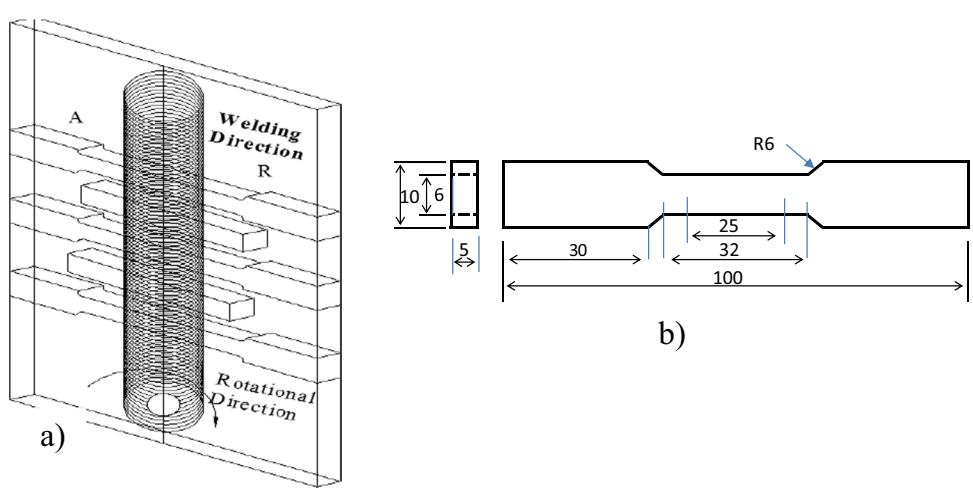

Fig. 2 Schematic representation of **a** FSW weld specimen and **b** specimen for UTS test

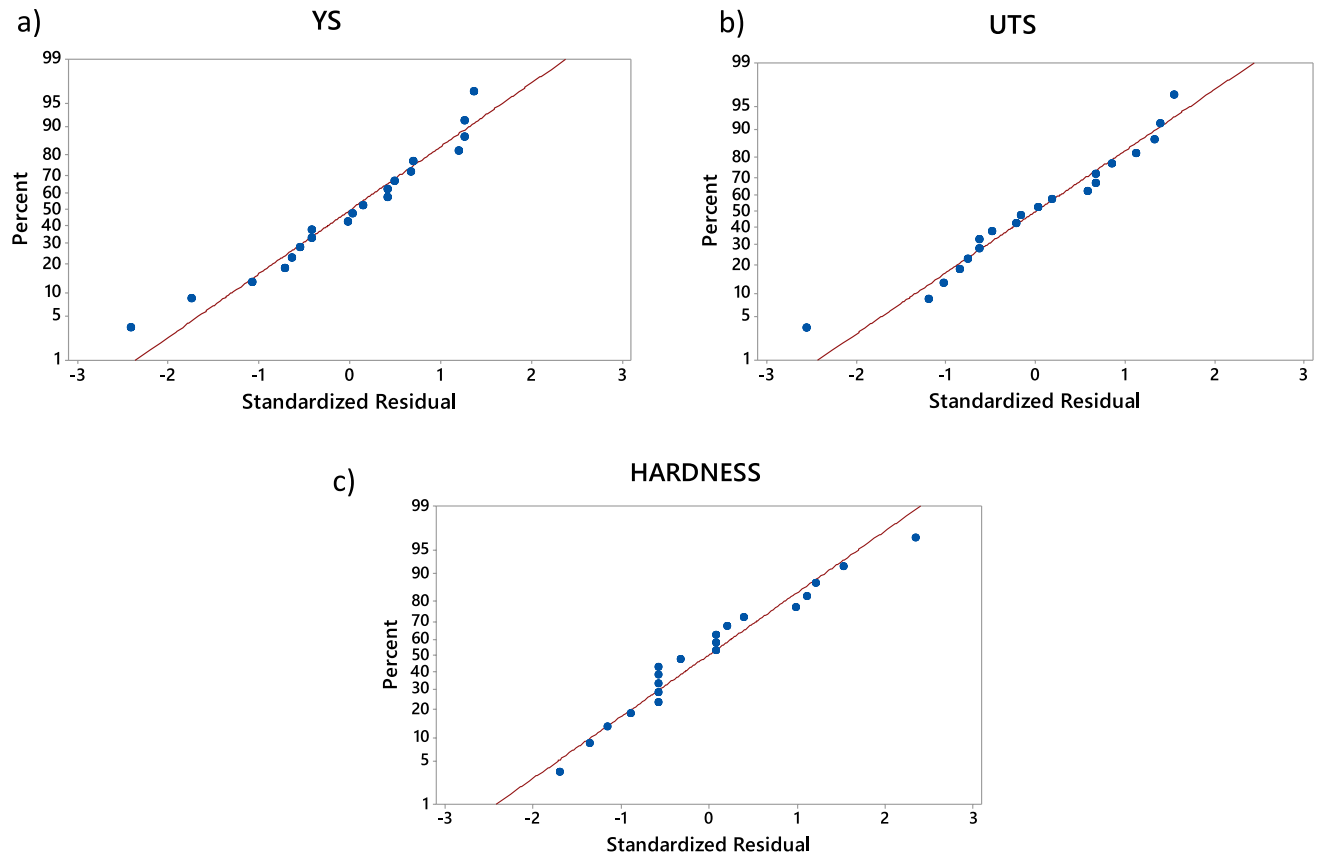

Fig. 3 Normal probability plot for **a** YS, **b** UTS, and **c** hardness

of ANOVA, which ensures the accuracy of the developed model. It has been observed that models developed for YS, UTS, and hardness are adequate since the measured F ratios are lesser than the computed values at a confidence level of 95%. Similarly, the values, R^2, and adjusted R^2 of the developed models are greater than 95%, which indicates that the regression models are adequate for further analysis. Figure 3a, b, and c show the normal probability plots in which standard residuals were plotted on X-axis, and Y-axis was plotted with normal percentage probability to find whether the data follows normal distribution [33]. Almost all points were within the acceptable range (normal observation range) except few points spotted slightly distant from the straight line which indicates that residuals are nearly aligned with the straight line and confirms that the errors follow normal distribution (http://www.itl.nist.gov/div898/handbook/prc/section1/prc16.html). The experimental and predicted data were compared and plotted as a scatter diagram for better understanding as depicted in Fig. 4a–c. Predicated values and experimental values are in close agreement, and the points are distributed around a straight line indicating the suitability of the mathematical model [34].

4 Results

The effect of each of the independent process variables on the dependent variables is depicted in Figs. 5a and b and 6, which confirms the interdependencies of the process parameters and the output responses.

4.1 Effect of tool traverse/welding speed

Figure 5a depicts the effect of tool traverse/welding speed on YS, UTS, and the hardness of the FS welded composites. It has been learned from the graph that an increase in the welding speed within the chosen range results in an increase in output response values. As observed in the trial runs, choosing welding speed beyond the chosen range leads to the welding defects such as voids, pinholes, and tunnel holes. Welding speed affects the duration of heat transfer in the weld region and thereby controls the rate of cooling. The joint shows lesser UTS at the lower welding speed due to the higher heat supply caused by the slow movement of the tool. Higher heat input and reduced cooling rate result in improper plasticization and turbulent material flow causing poor consolidation of the material in the weld region [35–37]. Hence, both YS and UTS of the joint show lesser

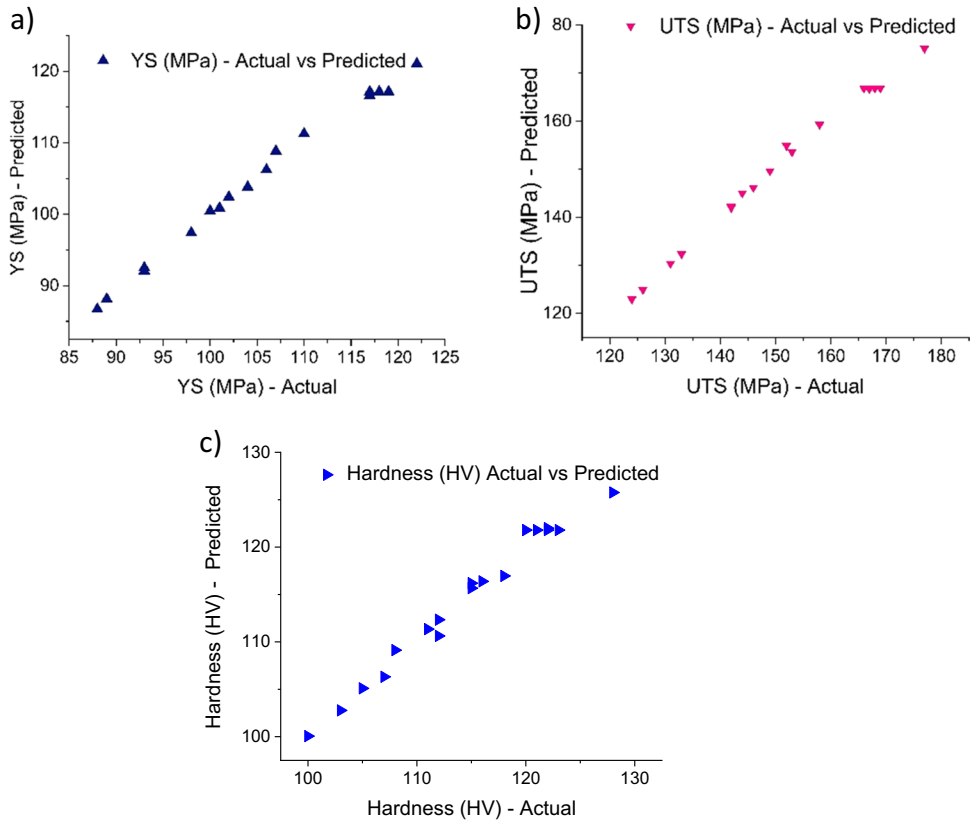

Fig. 4 Predicted vs actual responses for **a** YS, **b** UTS, and **c** hardness

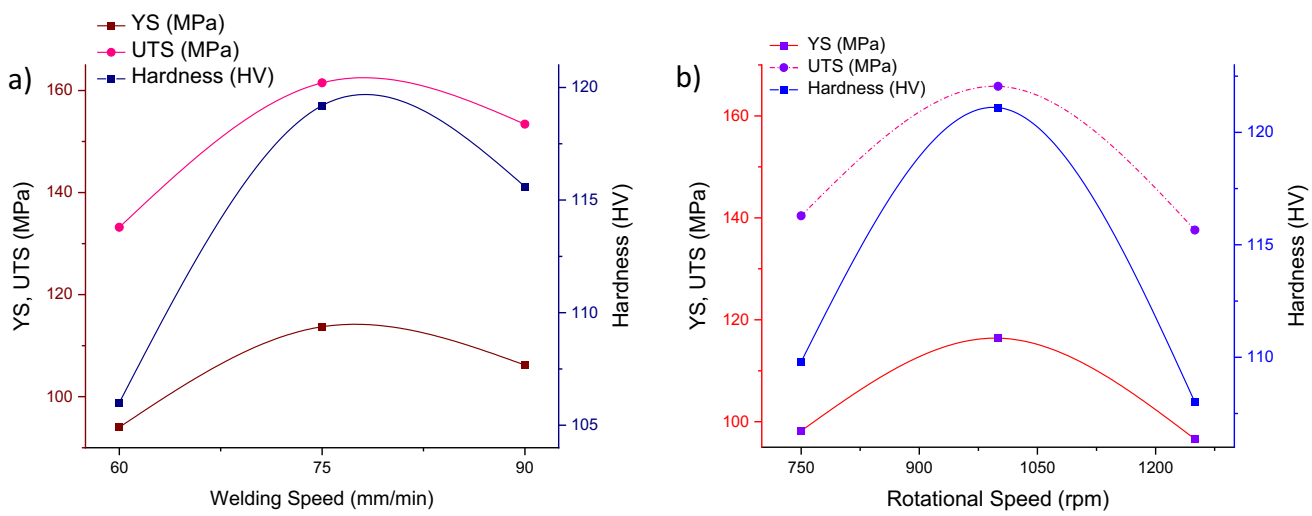

Fig. 5 Effect of **a** welding speed and **b** rotational speed on YS, UTS, and hardness

value at lower welding speed. The joint strength gradually increases as the welding speed increases due to the proper plasticization and smooth material flow resulting from the optimum heat input. Welding speed beyond the chosen range results in defects due to the poor plasticization and consolidation of the material.

The hardness of the joint shows a similar trend as shown by the UTS to welding speed. Non-uniform material flow and poor consolidation of the material reduce the hardness at lower welding speed, whereas joint exhibits higher hardness as the welding speed increases within the chosen speed range as it assists in proper plasticization, uniform flow, and improved consolidation of the material [37].

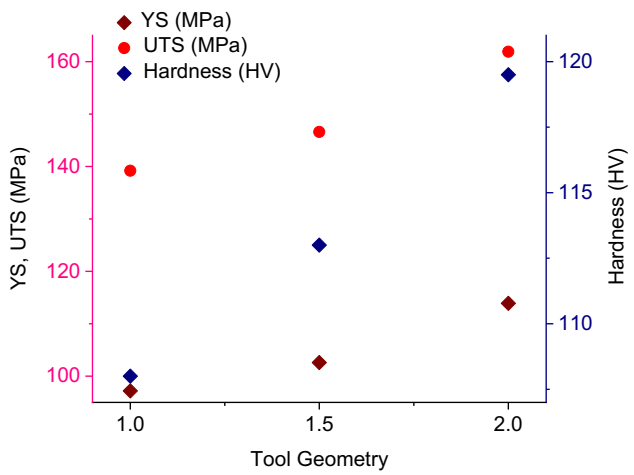

Fig. 6 Influence of tool geometry on UTS, YS, and hardness

4.2 Effect of tool rotational speed

Figure 5b depicts the average values of YS, UTS, and hardness values for different levels of tool rotational speeds. It has been found that initially YS, UTS, and hardness increase as the rotational speed increases, and a further increase in the speed reduces these values. These trends are in line with the reported literature, in which higher speed results in excessive heat supply at the weld zone [35, 36]. The almost parallel plots of YS and UTS in Fig. 5b indicate that the joints formed at different speeds show adequate ductility by exhibiting sufficient resistance for the propagation of cracks and preventing premature breakage of weld plate in the strain hardened zone. Similar results are observed in several other published literature [36, 38].

An increase in the tool rotational speed increases the hardness in the weld zone initially and thereafter decreases. Optimum rotational speed assists in uniform material flow in the weld zone and proper dispersion of reinforcement, thereby increasing the hardness, whereas increased rotational speed results in higher heat input as well as turbulent material flow resulting in improper consolidation of the material and thereby reduces the hardness.

4.3 Effect of tool pin geometry

Figure 6 shows the effect of tool geometry on the joint properties. The tool with a TC pin enables the smooth flow of material from top to bottom as well as from front to the rear side of the pin [36]. 2019). TC tool offers clean, smooth joints with better surface finish, whereas surface finish of the joint prepared with triangle and square pin was less compared to that obtained using TC tool. Mechanical properties of the joint prepared with the SQ tool show a better result followed by TL and TC tool, respectively [39]. The tool with sharp edges provides a pulsating effect during the welding process, which assists in proper stirring and better consolidation of the plasticized material. For the same speed, the SQ tool provides a 33% more pulsating effect than the TL tool and, hence, produces joints with better mechanical properties. From the performed experiments, it has been observed that joints produced with the SQ tool show improved joint properties compared to those obtained using the other two tool geometries for the same process parameter values.

5 Process optimization using TLBO algorithm

5.1 Working of TLBO algorithm

Inspired by the teaching and learning process, Rao et al. developed a TLBO algorithm for process optimization. TLBO follows the principle of "how teacher influences and enhances the output of a learner in the class" [25]. The algorithm consists of two vital components, namely teacher and learner. TLBO is based on two types of learning, one is through the teacher, and the other is through interaction among the learner known as the teacher phase and learner phase respectively. Being a population-based technique, a bunch of students (i.e., learners) is taken as the population in TLBO, and the subjects offered to the students are considered independent process parameters of the optimization problem. The results of the students are taken as the fitness value of the problem, which has to be optimized. Figure 7 depicts the flowchart of the working of the TLBO algorithm.

5.1.1 Level I—teacher level

At this level, the teacher tries to enhance the average results of the class in his subject. Assume there are "n" learners and "m" subjects. Let the learner be denoted by k, varying from 1 to n, and the subject is denoted by j, varying from 1 to m, and iteration is denoted by "i." At any iteration, the average result of the learner in a subject is represented by $M_{j,\,i}$. By considering all the subjects from the total learner population, the best overall results (i.e., $A_{total\text{-}kbest,\,i}$) are taken as the output/result of the best learner, denoted by k_{best}. The best learner is then renamed as a teacher in the algorithm, as a teacher is usually a better-learned person. The difference between the average

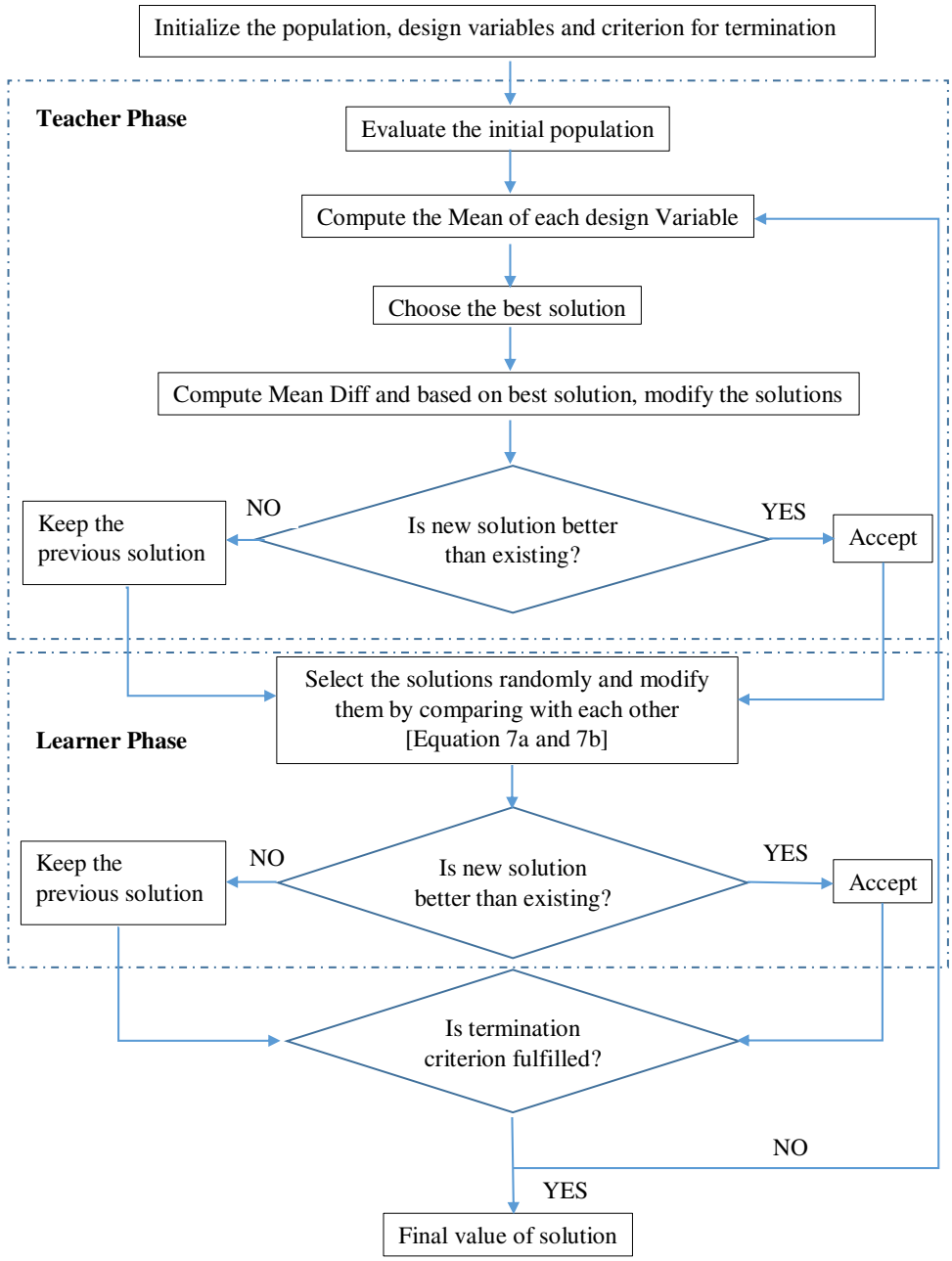

Fig.7 Flow chart of TLBO algorithm [20]

result of a learner in each subject and the value corresponding to the best learner (i.e. teacher) is presented as:

$$MeanDiff_{j,k,i} = r_i(A_{j,kbest,i} - T_F M_{j,i}) \tag{4}$$

where $A_{j,kbest,i}$ is the result of the best learner in the subject/variable "j," r_i represents random number within the interval of 0 and 1, and T_F is the teaching factor and it takes values either 1 or 2. Value of the T_F is calculated by:

$$T_F = round[1 + rand(0,1)\{2-1\}] \tag{5}$$

The prevailing solution is revised based on the $MeanDiff_{j,k,i}$ in the teacher phase as per the below equation.

$$A'_{j,k,i} = A_{j,k,i} + MeanDiff_{j,k,i} \tag{6}$$

Here, $A'_{j,k,i}$ is the revised value of $A_{j,k,i}$. Finally, accept $A'_{j,k,i}$ if it provides a higher function value. All these values are maintained and transferred to the learner level as input values at the end of the teacher level.

5.1.2 Learner level

Usually, by interacting among themselves, learners enhance their knowledge. For the given size of population "n," the learning process in this level is formulated as follows:

Table 4 TLBO algorithm predictions and the experimental values

Response function optimized	TLBO algorithm estimations				Experimental values				Error %
	FSW process variables			Response value	FSW process variables			Response values	
	RS	WS	TG		RS	WS	TG		
YS	987.425	89.996	1.729	121.7323	1000	90	2	120	1.443
UTS	989.024	89.999	1.741	176.0498	1000	90	2	174	1.178
Hardness	997.244	89.999	1.819	126.6664	1000	90	2	126	0.529

Choose any two learners F and G randomly, such that $A'_{total-F,i} \neq A'_{total-G,i}$ (where $A'_{total-F,i}$ and $A'_{total-G,i}$ are the revised values of $A_{total-G,i}$ and $A_{total-G,i}$, respectively, at the end of the previous level).

$$A''_{j,F,i} = A'_{j,F,i} + r_i\left(A'_{j,F,i} - A'_{j,G,i}\right), \text{ if } A'_{total-F,i} < A'_{total-G,i} \tag{7a}$$

$$A''_{j,F,i} = A'_{j,F,i} + r_i\left(A'_{j,G,i} - A'_{j,F,i}\right), \text{ if } A'_{total-F,i} > A'_{total-G,i} \tag{7b}$$

Accept $A''_{j,F,i}$ if the function value provided by this is better than the previous condition.

MATLAB R2019b software was used to develop the TLBO algorithm. TLBO requires the only size of the population and the total number of iterations to develop the algorithm [40]. The size of the population for the current study was fixed as 20 and the number of iteration as 50. The result of the TLBO used in the present problem is shown in Table 4.

5.2 Validation

An optimal combination of FSW process variables was obtained from Eqs. 3(a), 3(b), and 3(c), for output responses YS, UTS, and hardness, respectively, using the TLBO algorithm. Confirmation tests were performed to validate the results. Three friction stir weld samples were prepared using a close range of process variables obtained from the TLBO algorithm to validate its performance. Table 4 compares the output responses obtained from the TLBO algorithm with the response values obtained from the experiments. As three samples were prepared to have a close range of process parameters, the mean value of each of the output responses was considered for comparison with estimated response values. From the confirmation test, it can be confirmed that the developed models are acceptable to optimize the FSW process variable values to join AA6061/TiO_2 composite, using the TLBO algorithm.

6 Conclusion

The effect of FSW process variables and their interactions was determined in TiO_2-reinforced aluminum matrix composite FSW joints, and the mathematical relationships were established for output responses in terms of independent input process variables. The accuracy of the mathematical models was tested using ANOVA. Models developed for YS, UTS, and hardness are satisfactory as the measured F ratios are lesser than the computed results at a 95% level of confidence; similarly, the values, R^2, and adjusted R^2 indicate that the models are passable enough for further analysis. Further, the TLBO algorithm was employed to optimize the FSW process parameters within the selected range, and the results of the algorithm were experimentally verified.

The current study revealed that an increase in tool rotational speed improves the UTS, YS, and hardness initially and attains a maximum value. However, as the rotational speed increases beyond a certain value, the response values decrease gradually, whereas an increase in the welding speed increases the response values within the chosen range of welding speed. The tool with a square pin provides a better response compared to other tool geometries due to the pulsating effect and enhanced stirring of the material. UTS of 174 MPa, yield strength of 120 MPa, and hardness of 126HV have been obtained by using the optimized experimental condition provided by the TLBO technique. The present work also confirms that the developed empirical model and optimization of the process by TLBO is a reliable and favorable technique to predict the optimal combination of FSW process variables to weld composites that yield the best joint properties.

Funding Open access funding provided by Manipal Academy of Higher Education, Manipal.

Open Access This article is licensed under a Creative Commons Attribution 4.0 International License, which permits use, sharing, adaptation, distribution and reproduction in any medium or format, as long as you give appropriate credit to the original author(s) and the source, provide a link to the Creative Commons licence, and indicate if changes were made. The images or other third party material in this article are included in the article's Creative Commons licence, unless indicated otherwise in a credit line to the material. If material is not included in

the article's Creative Commons licence and your intended use is not permitted by statutory regulation or exceeds the permitted use, you will need to obtain permission directly from the copyright holder. To view a copy of this licence, visit http://creativecommons.org/licenses/by/4.0/.

References

1. Storjohann D, Barabash OM, David SA et al (2005) Fusion and friction stir welding of aluminum-metal-matrix composites. Metall Mater Trans A 36:3237–3247. https://doi.org/10.1007/s11661-005-0093-4
2. Meng X, Huang Y, Cao J et al (2021) Recent progress on control strategies for inherent issues in friction stir welding. Prog Mater Sci 115:100706. https://doi.org/10.1016/j.pmatsci.2020.100706
3. Thomas WM, Nicholas D, Needham JC, Murch MG, Templesmith P, Dawes CJ (1991) Friction stir welding, International Patent Application No. PCT/GB92/02203, 1991
4. Mishra RS, Mahoney MW, Sato Y, Hovanski Y (2016) Friction stir welding and processing VIII. Frict Stir Weld Process VIII 50:1–300. https://doi.org/10.1007/978-3-319-48173-9
5. Huang Y, Xie Y, Meng X et al (2018) Numerical design of high depth-to-width ratio friction stir welding. J Mater Process Technol 252:233–241. https://doi.org/10.1016/j.jmatprotec.2017.09.029
6. Prikhodko SV, Savvakin DG, Markovsky PE et al (2021) Friction welding of conventional Ti-6Al-4V alloy with a Ti-6Al-4V based metal matrix composite reinforced by TiC. Weld World 65:415–428. https://doi.org/10.1007/s40194-020-01025-8
7. Huang Y, Wan L, Si X et al (2019) Achieving high-quality al/steel joint with ultrastrong interface. Metall Mater Trans A Phys Metall Mater Sci 50:295–299. https://doi.org/10.1007/s11661-018-5006-4
8. Avettand-Fènoël MN, Simar A (2016) A review about friction stir welding of metal matrix composites. Mater Charact 120:1–17. https://doi.org/10.1016/j.matchar.2016.07.010
9. Prabhu S, Shettigar AK, Herbert MA, Rao SS (2019) Microstructure evolution and mechanical properties of friction stir welded AA6061/Rutile composite. Res. Express, Mater. https://doi.org/10.1088/2053-1591/ab0f4e
10. Salih OS, Ou H, Sun W, McCartney DG (2015) A review of friction stir welding of aluminium matrix composites. Mater Des 86:61–71. https://doi.org/10.1016/j.matdes.2015.07.071
11. Prabhu SR, Shettigar AK, Herbert MA, Rao SS (2019) Microstructure and mechanical properties of rutile-reinforced AA6061 matrix composites produced via stir casting process. 29:2229–2236. https://doi.org/10.1016/S1003-6326(19)65152-6
12. Heidarzadeh A, Mironov S, Kaibyshev R et al (2020) Friction stir welding/processing of metals and alloys: a comprehensive review on microstructural evolution. Prog Mater Sci 117:100752. https://doi.org/10.1016/j.pmatsci.2020.100752
13. Buffa G, Fratini L, Micari F (2012) Mechanical and microstructural properties prediction by artificial neural networks in FSW processes of dual phase titanium alloys. J Manuf Process 14:289–296. https://doi.org/10.1016/j.jmapro.2011.10.007
14. Siva S, Sampathkumar S, Sudha J, Tamilprabakaran S (2019) Optimization and characterization of friction stir welded NAB alloy using multi-criteria decision-making approach. Mater Res Express 6. https://doi.org/10.1088/2053-1591/ab23b4
15. Kalaiselvan K, Murugan N (2012) Optimizations of friction stir welding process parameters for the welding of Al-B4C composite plates using generalized reduced gradient method. Procedia Eng 38:49–55. https://doi.org/10.1016/j.proeng.2012.06.008
16. Verma S, Gupta M, Misra JP (2019) Optimization of process parameters in friction stir welding of armor-marine grade aluminium alloy using desirability approach. Mater Res Express 6. https://doi.org/10.1088/2053-1591/aaea01
17. Renani HK, Mirsalehi SE (2019) Optimization of FSW lap joining of pure copper using Taguchi method and grey relational analysis. Mater Res Express 6(5):056525. https://doi.org/10.1088/2053-1591/ab021d
18. Prabhu SR, Shettigar A, Herbert M, Rao S (2018) Multi response optimization of friction stir welding process variables using TOPSIS approach, in IOP Conference Series: Materials Science and Engineering. https://doi.org/10.1088/1757-899X/376/1/012134
19. Maboud AAGA, El-Mahallawy NA, Zoalfakar SH (2018) Process parameters optimization of friction stir processed Al 1050 aluminum alloy by response surface methodology (RSM). Mater Res Express 6(2):026527. https://doi.org/10.1088/2053-1591/aaed7c
20. Sreenivasan KS, Satish Kumar S, Katiravan J (2019) Genetic algorithm-based optimization of friction welding process parameters on AA7075-SiC composite. Eng Sci Technol Int J 22:1136–1148. https://doi.org/10.1016/j.jestch.2019.02.010
21. Parida B, Pal S (2015) Fuzzy assisted grey Taguchi approach for optimization of multiple weld quality properties in friction stir welding process. Sci Technol Weld Join 20:35–41. https://doi.org/10.1179/1362171814Y.0000000251
22. Shojaeefard MH, Behnagh RA, Akbari M et al (2013) Modelling and Pareto optimization of mechanical properties of friction stir welded AA7075/AA5083 butt joints using neural network and particle swarm algorithm. Mater Des 44:190–198. https://doi.org/10.1016/j.matdes.2012.07.025
23. Prasanth RSS, Hans Raj K (2018) Determination of optimal process parameters of friction stir welding to join dissimilar aluminum alloys using artificial bee colony algorithm. Trans Indian Inst Met 71:453–462. https://doi.org/10.1007/s12666-017-1176-9
24. Pawar PJ, Rao RV (2013) Parameter optimization of machining processes using a teaching-learning-based optimization algorithm. Int J Adv Manuf Technol 67:995–1006. https://doi.org/10.1007/s00170-012-4524-2
25. Rao RV, Savsani VJ, Vakharia DP (2012) Teaching-learning-based optimization: an optimization method for continuous non-linear large-scale problems. Inf Sci (NY) 183:1–15. https://doi.org/10.1016/j.ins.2011.08.006
26. Rao RV, Savsani VJ, Vakharia DP (2011) Teaching-learning-based optimization: a novel method for constrained mechanical design optimization problems. CAD Comput Aided Des 43:303–315. https://doi.org/10.1016/j.cad.2010.12.015
27. Montgomery DC (2017) Design and analysis of experiments. Wiley
28. Montgomery DC, Runger GC (2014) Applied statistics and probability for engineers. Wiley
29. Khalkhali A, Ebrahimi-Nejad S, Malek NG (2018) Comprehensive optimization of friction stir weld parameters of lap joint AA1100 plates using artificial neural networks and modified NSGA-II. Mater Res Express 5. https://doi.org/10.1088/2053-1591/aac6f6
30. Reddy TA (2011) Applied data analysis and modeling for energy engineers and scientists. Springer Science & Business Media

31. Cochran WG, Cox GM (1992) Experimental design. 2nd ed. Wileys
32. Minitab I (2010) Minitab 16 statistical software. URL: [Computer software]. Minitab, Inc., State College (www.Minitab.com)
33. Chambers JM (2018) Graphical methods for data analysis. CRC Press
34. Kumar SS, Murugan S, Ramachandran KK (2019) Identifying the optimal FSW process parameters for maximizing the tensile strength of friction stir welded AISI 316L butt joints. Meas J Int Meas Confed 137:257–271. https://doi.org/10.1016/j.measurement.2019.01.023
35. Prabhu S, Shettigar AK, Rao K, Rao S, Herbert M (2016) Influence of welding process parameters on microstructure and mechanical properties of friction stir welded aluminium matrix composite. Mater Sci Forum 880:50–53. https://doi.org/10.4028/www.scientific.net/msf.880.50
36. Salih OS, Ou H, Wei X, Sun W (2019) Microstructure and mechanical properties of friction stir welded AA6092/SiC metal matrix composite. Mater Sci Eng A 742:78–88. https://doi.org/10.1016/j.msea.2018.10.116
37. Liu H, Hu Y, Zhao Y, Fujii H (2015) Microstructure and mechanical properties of friction stir welded AC4A+30vol.%SiCp composite. Mater Des 65:395–400. https://doi.org/10.1016/j.matdes.2014.09.014
38. Li YZ, Wang QZ, Xiao BL, Ma ZY (2018) Effect of welding parameters and B4C contents on the microstructure and mechanical properties of friction stir welded B4C/6061Al joints. J Mater Process Technol 251:305–316. https://doi.org/10.1016/j.jmatprotec.2017.08.028
39. Vijay SJ, Murugan N (2010) Influence of tool pin profile on the metallurgical and mechanical properties of friction stir welded Al-10wt.% TiB2 metal matrix composite. Mater Des 31:3585–3589. https://doi.org/10.1016/j.matdes.2010.01.018
40. Venu B, Suvarna Raju L, Venkata Rao K (2020) Multiobjective optimization of friction stir weldments of AA2014-T651 by teaching–learning-based optimization. Proc Inst Mech Eng C J Mech Eng Sci 234:1146–1155. https://doi.org/10.1177/0954406219891755

Publisher's note Springer Nature remains neutral with regard to jurisdictional claims in published maps and institutional affiliations.